Percolation disorder in chromatographic systems

LETTER TO THE EDITOR

Percolation disorder in chromatographic systems

J S Andrade Jr and K Rajagopal

Programa de Engenharia Química, COPPE, Universidade Federal do Rio de Janeiro, CP 68502, Rio de Janeiro, RJ, Brazil

Abstract. A pore space model is presented to describe the transport of mass within pore packings of chromatographic columns. The particle pore structure is conceptually represented by a network of capillaries subjected to bond percolation disorder. The efficiency of the system is assessed in terms of a mass dispersivity factor (h) which accounts for the band broadening of the peak response. The results show a large dispersivity at a percolation fraction near the threshold which reflects the critical properties of the structure with respect to connectivity and tortuosity.

It was only recently that the percolation concepts [1] became a useful tool to quantify the effect of topological disorder on transport phenomena in porous media. Percolation networks of capillaries have been successfully used to describe the problem of diffusion and reaction in porous catalysts [2–5] as well as dispersion in disordered composites [6–8].

In the work of Charlaix *et al* [9], the *capacitance* model of Coats and Smith [10] has been applied to describe *anomalous* dispersion curves obtained from experiments with consolidated porous media. This classical model is a modified version of the traditional convection-diffusion equation which considers the flow of fluid through a packed bed with *stagnant* pockets of fluid acting as dead spaces. Recent works by McGreavy *et al* [11] and Andrade *et al* [12] are directed to the representation of *chromatographic packings* in terms of a network conceptualization for the structure of the pellet. The model combines the Coats–Smith and network of pore approaches and a detailed description of the microscopic phenomenology enables the diffusional mechanism of mass transport to be evaluated at the capillary level of the particle in the packing. The results show a very strong influence of the pore structure on the macroscopic response of the system. In this letter, we briefly introduce the methodology developed by Andrade *et al* [12] which allows for bond percolation disorder in the network model of the particle pore space. From the results of computational simulations, the overall efficiency of the column is then analysed as a function of the allowed fraction of pores in the network (p), a structural parameter.

As shown in figure 1, the porous particles of uniform size (l_P) are structurally represented by a two-dimensional square network. Cylindrical pores of constant length (l) and radius (R) are randomly connected to sites of negligible volume according to the percolation fraction (p). Figure 2(a) shows the lattice representation of the pore network with the nodal enumeration scheme adopted in this formulation. The following
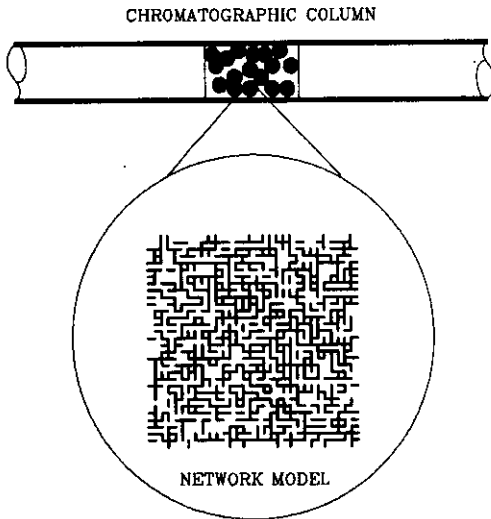
Figure 1. Chromatographic column with porous particles represented by a typical percolation network.
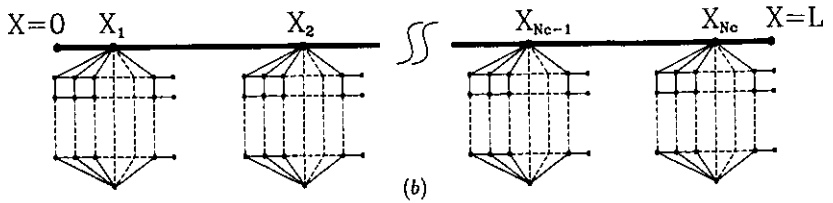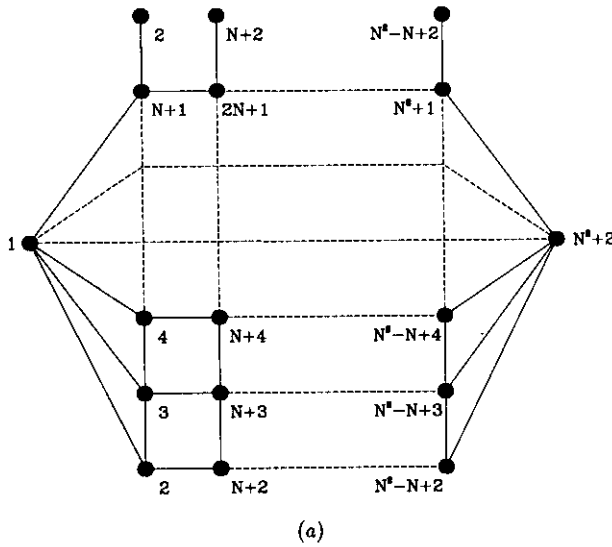

(a)

(b)

Figure 2. (*a*) Lattice representation of the particle with nodal enumeration scheme. Periodic boundary conditions are used to reduce the effect of finite size in the transverse direction. (*b*) Orthogonal collocation technique with network of pores.

mass balance describes the diffusive transport of a tracer inside a typical pore between adjacent nodes $\{i\}$ and $\{j\}$:

$$\frac{\partial c}{\partial t} = D_m \frac{\partial^2 c}{\partial x^2} \tag{1}$$

with the following initial and boundary conditions:

$$c(x, 0) = 0$$
$$c(0, t) = c_{\{i\}} \tag{2}$$
$$c(l, t) = c_{\{j\}}$$

where $c(x, t)$ is the tracer concentration in the capillary, x is the capillary axial coordinate and D_m is the tracer molecular diffusivity. The molar flux of the tracer into a pore from adjacent sites $\{i\}$ and $\{j\}$ is given by:

$$J_{\{i,j\}} = -\pi R^2 D_m \left(\frac{dc}{dx} \bigg|_{x=0} \right)_{\{i,j\}} . \tag{3}$$

Considering the nodes as perfect mixing points with no tracer accumulation, a mass conservation equation can be expressed for node $\{i\}$ as:

$$\sum_{j \in (i)} J_{\{i,j\}} = 0 \tag{4}$$

where (i) makes reference to the set of i-adjacent sites which are connected to the site $\{i\}$.

A mass balance in the tracer concentration at the mobile phase of the column $(C_m(X, t))$ gives:

$$D_L \frac{\partial^2 C_m}{\partial X^2} - \langle v \rangle \frac{\partial C_m}{\partial X} - \frac{\partial C_m}{\partial t} - \frac{(1 - \varepsilon_C)\varepsilon_P}{\varepsilon_C V_{PS}} \sum_{j=2}^{N+1} J_{\{1,j\}} = 0 \tag{5}$$

with the following initial and boundary conditions for the entrance $(X = 0)$ and exit $(X = L)$ of the column:

$$C_m(X, 0) = 0$$

$$\langle v \rangle \delta(t) = \langle v \rangle C_m(0, t) - D_L \frac{\partial C_m}{\partial X} \bigg|_{x=0} \tag{6}$$

$$\frac{\partial C_m}{\partial X} \bigg|_{X=L} = 0$$

where X is the column axial coordinate, D_L is the dispersion coefficient, $\langle v \rangle$ is the interstitial velocity of the mobile phase and $\delta(t)$ is the Dirac function representing a pulse of unitary strength in concentration at the column inlet. In the summation term of equation (5) the subscripts refer to the capillaries at the network entry (see figure 2(a)), N is the network dimension, V_{PS} is the pore space volume and ε_P and ε_C are the particle and the column porosities respectively. The factor $(1 - \varepsilon_C)\varepsilon_P / \varepsilon_C V_{PS}$ corresponds to the reciprocal of the external fluid volume surrounding a single particle in the mobile phase. The relation between the mobile phase and the pores in the pellet surface can be specified by assuming that the resistance to mass transfer is negligible at the fluid film surrounding the external surface of the particle:

$$C_m = c_{\{1\}} . \tag{7}$$

From the Laplace transform solution of equations (1) and (2), the transformed form of $J_{(i,j)}$ can then be expressed as a linear function of the two terminal transformed concentrations at the connected nodal points [11–12]:

$$\bar{J}_{(i,j)} = \pi R_{(i,j)}^2 (D_m \sigma)^{1/2} \left[\frac{\bar{c}_{(i)}}{\tanh(\alpha l)} - \frac{\bar{c}_{(j)}}{\sinh(\alpha l)} \right] \tag{8}$$

where $\alpha = (\sigma/D_m)^{1/2}$ and σ is the Laplace transform variable. This expression can be introduced in the transformed form of equation (4) and applied to each nodal point to generate a set of coupled linear algebraic equations in the transformed nodal concentrations. The transformed version of equation (5) is then discretized by means of orthogonal collocation as schematically demonstrated in figure 2(b) (see reference [11] for numerical details). The dependence of the flux summation term in equation (5) on the macroscopic coordinate X is consistently considered in the numerical technique by connecting the network of pores to each of the selected orthogonal collocation points at the axial direction in the mobile phase. The final mathematical representation of the model can then be written as:

$$A(\sigma)c(\sigma) = b \tag{9}$$

where c is the vector of transformed nodal concentrations, b is a vector obtained from equation (6) and A is a matrix corresponding to the coupling between the nodal mass balances and the orthogonal collocation coefficients [11].

The matrix expansion technique presented by Koplik *et al* [7] is adopted here for the computation of the transit-time moments of the column residence time distribution. From the peak retention time (μ) and variance (σ^2) at the column exit ($X = L$), a dimensionless mass dispersivity factor (h) can be calculated as:

$$h = \sigma^2/\mu^2. \tag{10}$$

This composite index is a cumulative description of the overall mass transport in the system. For a given value of p, simulations have been performed with 100 *realizations* of 30×30 networks to produce average values of h which are representative of the pore structure. The parameters employed in the simulations are listed in table 1. Figure 3 shows the dependence of h on the fraction of allowed bonds (p) in the lattice. At the percolation limit of $p = 0.0$ the capillaries are absent (non-porous packing) and at $p = 1.0$ the network of pores is complete (well connected structure). One would obviously expect a higher mass dispersivity at $p = 1.0$ than at $p = 0.0$ which is compatible with the results shown in figure 3. The interesting feature about these simulations is a large value of h at $p = \frac{1}{2}$ which is also associated with a large uncertainty arising from the sampling procedure. Similar anomalies have already been predicted [7–8, 13–15] and experimentally observed [9, 14–16] for the dispersion of systems with stagnant zones of percolation geometry. This p value is the bond percolation threshold for

Table 1. Parameters employed in the simulations.

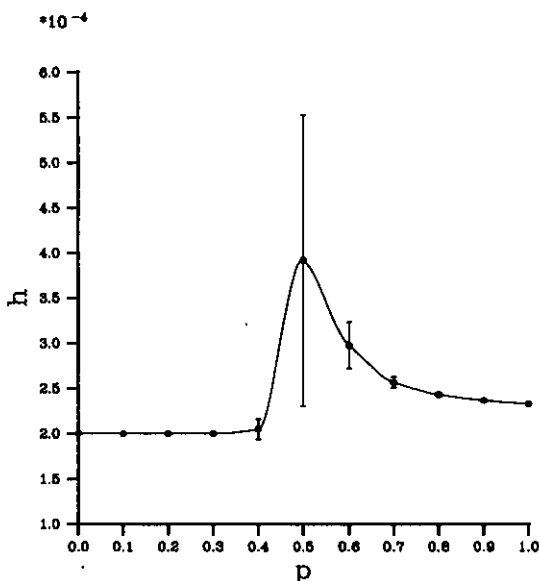|	
Peclet number ($Pe = \langle v \rangle L/D_L$)	10^4
β ($= \langle v \rangle l_P^2/LD_m$)	10^{-4}
column voidage (ε_C)	0.5
particle porosity (ε_P)	0.5
capillary length (l)	$l_P/(N+1)$
pore radius (R)	$l/10$

Figure 3. Dependence of h on the fraction of allowed pores (p) in the network.

square networks of infinite size [17] and network configurations generated with this critical percolation fraction are in the vicinity of a sudden change in connectivity. As a consequence, pore pathways terminated by dead-end pores are very long and tortuous at this p value, and a maximum mass dispersivity (h) is observed. The wide fluctuations at this transition point can be explained in terms of the relatively small network dimension used in the simulations for reasons of computational feasibility. However, it does not compromise the qualitative aspect of the results and somehow emphasizes the *critical nature* of the threshold topology.

In summary, a modelling technique has been devised in this work which allows the effect of topological disorder in the pore packing on the resolution of chromato-graphic systems to be investigated. The percolation process proved to be the natural method for describing this structural influence since it provides a systematic way of performing changes in the connectivity and tortuosity of the particle pore space. The results demonstrate a significant increase in the column band broadening at a bond percolation fraction near the threshold. In design or selection of chromatographic packings this fact might be taken into consideration since it reflects negatively on the performance of the system. It also reinforces the potentialities of chromatography as a practical tool for topological identification and characterization of disordered pore structures.

References

[1] Stauffer D *Introduction to Percolation Theory* (London: Taylor and Francis)
[2] Sahimi M and Tsotsis T T 1985 *J. Catal.* **96** 552

[3] Mohanty K K, Ottino J M and Davis H T 1982 *Chem. Eng. Sci.* **37** 905
[4] Mo W T and Wei J 1986 *Chem. Eng. Sci.* **41** 703
[5] Sahimi M, Gavalas G R and Tsotsis T T 1990 *Chem. Eng. Sci.* **45** 1443
[6] Sahimi M, Hughes B D, Scriven L E and Davies H T 1986 *Chem. Eng. Sci.* **41** 2103
[7] Koplik J, Redner S and Wilkinson D 1988 *Phys. Rev.* A **37** 2619
[8] Roux S and Guyon E 1987 *Europhys. Lett.* **4** 175
[9] Charlaix E, Hulin J P and Plona T J 1987 *Phys. Fluids* **30** 1690
[10] Coats K H and Smith B D 1964 *Soc. Pet. Eng. J. AIME* **231** 73
[11] McGreavy C, Andrade J S Jr and Rajagopal K 1990 *Chromatographia* **30** 639
[12] Andrade J S Jr, Rajagopal K and McGreavy C 1991 *Chromatographia* in press
[13] de Gennes P G 1983 *J. Fluid Mech.* **136** 189
[14] Gist G A, Thompson A H, Katz A J and Higgins R L 1990 *Phys. Fluids* A **2** 1533
[15] Bacri J-C, Rosen M and Salin D 1990 *Europhys. Lett.* **11** 127
[16] Bacri J-C, Rakotomalala N and Salin D 1987 *Phys. Rev. Lett.* **58** 2035
[17] Kesten H 1980 *Commun. Math. Phys.* **41** 74